

Activation of ground granulated blast furnace slag by using calcined dolomite

Kai Gu^{1,2,*}, Fei Jin², Abir Al-Tabbaa², Bin Shi¹

¹ School of Earth Sciences and Engineering, Nanjing University, 163 Xianlin Avenue, Nanjing, China, 210093

² Department of Engineering, University of Cambridge, Trumpington Road, Cambridge, UK, CB2 1PZ

*Corresponding author: gukainju@gmail.com

ABSTRACT: Both reactive MgO and CaO are alternative activators for ground granulated blast furnace slag (GGBS). In this study natural dolomite, as a source of MgO and CaO, was calcined at 800°C (D800) and 1000°C (D1000) under air. The activation of GGBS with the calcined dolomites was investigated using compressive tests, pH measurement of pore solutions, powder X-ray diffraction (XRD) and thermogravimetric analysis (TGA). The results indicated that both calcined dolomites can effectively activate GGBS. D800 showed a relatively slower acceleration to GGBS than D1000 and both were slower than CaO. The use of D800 produced similar compressive strengths as did D1000 after 7 days curing but lower strengths at later ages. By increasing the dosage of activators, significantly higher strengths were obtained using D800 while only small increases were observed using D1000. The detected hydration products by XRD and TGA were mainly C-S-H and hydrotalcite-like phases, similar to those from other alkali-activated slags. The comparison to other activators indicated that using calcined dolomite can induce faster hydration of slag than using reactive MgO in the early age while slower than Portland cement in this study.

Key words: Alkali-activated slag; Dolomite; Calcination; Hydration

1. Introduction

The pursuit of more sustainable and environmental friendly construction materials to reduce

1 the use of ordinary Portland cement (OPC), which is associated with high energy consumption and
2
3 global greenhouse gas emission [1,2], has lasted for decades. By re-using industrial by-product blast
4
5 furnace slag, alkali-activated slag (AAS) is one of the most promising precursors in large scale
6
7 production and shows a huge potential to replace OPC [3], although still faces hurdles. Extensive
8
9 studies have suggested that the advantages of AAS include the development of earlier and higher
10
11 mechanical strengths [4–6], better resistance of chemical attack [7–9], stronger aggregate-matrix
12
13 interface formation [10,11], and lower heat of hydration [12,13].
14
15
16
17
18
19

20 The most commonly used alkali activators for AAS are sodium hydroxide, sodium silicate,
21
22 sodium carbonate and potassium hydroxide [14]. It is generally agreed that the mixture of sodium
23
24 hydroxide with sodium silicate is the most effective activator and provides the best formulation for
25
26 high strength and other advantageous properties. However, most of these activators do not exist
27
28 naturally and require energy intensive manufacturing processes [12,14], making them less
29
30 economical efficiency. In addition, some issues such as the fast setting time, the high drying
31
32 shrinkage, the highly corrosive nature of alkali solution, the viscosity of alkali solution and the heat
33
34 released by the dissolution of the alkali compounds, especially alkali hydroxide, during preparation
35
36 of the solutions should be carefully considered when using these activators [3,4,15–17]. These
37
38 **problems** have led researchers to pursue alternative effective activators or additives. Among others,
39
40 calcium hydroxide [Ca(OH)₂] and calcium oxide (CaO) are potential alternatives to alkali activators,
41
42 either as additives or main activators, due to their lower cost and durability enhancement [12,14,18].
43
44 It has been reported that Ca(OH)₂, as an additive, can increase the early strength (<7 days) of AAS
45
46 whilst later strength might be slightly reduced [19]. Collins and Sanjayan [5] found that AAS
47
48 concrete activated by a combination of sodium silicate and Ca(OH)₂ demonstrated considerably
49
50
51
52
53
54
55
56
57
58
59
60
61
62
63
64
65

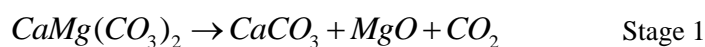
1 better workability and higher strength than concrete activated by a NaOH and Na₂CO₃ mixture.

2
3 When Ca(OH)₂ is used as a main activator, with different auxiliary activators (Na₂SO₄ and Na₂CO₃),
4
5
6 the activated slag concrete displays enhanced workability, delayed setting time and a similar
7
8
9 increasing rate of compressive strength to PC concrete [20]. The comparison between the effect of
10
11
12 CaO and Ca(OH)₂ in activating slag revealed that the use of CaO demonstrated a superior potential
13
14
15 for the activation of GGBS and produced a higher mechanical strength than Ca(OH)₂ [18].

16
17 More recently, some investigations have indicated that reactive magnesium oxide (MgO)
18
19
20 could also serve as an effective activator for GGBS, showing its advantages in the generation of
21
22
23 more voluminous hydration products than C-S-H gel therefore providing a more compacted
24
25
26 microstructure [21–24]. The results by Yi et al. [24] showed that the reactive MgO activated GGBS
27
28
29 achieved higher 28-day compressive strength than that of the equivalent Ca(OH)₂-GGBS system
30
31 due to the larger content of the voluminous hydrotalcite-like phases formed. The reason may be the
32
33
34 better pore filling effect of hydrotalcite-like phases. Considering the slow hydration in the early age
35
36
37 of reactive MgO activated slag and the limited global MgO production, the properties of slag pastes
38
39
40 activated with MgO-CaO mixtures with various MgO to CaO ratios by weight were investigated by
41
42
43 Gu [25]. That study found that the use of a small amount of CaO (MgO/CaO=19/1 by weight) could
44
45
46 significantly accelerate the early hydration of MgO-slag without sacrificing the long-term strength.
47
48
49 In addition, when the MgO/CaO ratio was ≤1 by weight, only a small difference in compressive
50
51
52 strengths of pastes was observed.

53 Dolomite is a naturally occurring mineral with abundant reserves around the world (i.e.
54
55
56 North America, northwestern and southern Europe, north and west Africa, the Middle East, and the
57
58
59 Far East [26]). In China, dolomite reservoirs in Liaoning, Neimenggu, Shanxi, Jiangsu, Fujian,
60
61
62
63
64
65

1 Hunan, Hubei and Guangxi were found, with reserves over 4 billion tons [27]. The thermal
2
3 decomposition of dolomite includes two stages [28–30]:
4



11 where the second stage usually takes place at higher temperature. Calcined dolomite may therefore
12 consist of MgO, CaO, CaCO₃ and possibly MgCO₃ and their proportions would vary depending on
13 the calcination temperature. Nevertheless, calcined dolomite can be considered as a potential source
14 of MgO-CaO blends as activators for slags.
15
16
17
18
19
20
21

22 The objective of this paper is to explore the use of calcined dolomite in the activation of GGBS.
23
24 Two calcined dolomite samples produced under different temperatures were investigated. The
25 performance of the different calcined dolomite activated slag pastes were then compared using
26 compressive tests, pH measurement of pore solutions, powder X-ray diffraction (XRD) and
27 thermogravimetric analysis (TGA). In addition, CaO activated slag paste was prepared as a
28 reference.
29
30
31
32
33
34
35
36
37
38

39 2. Materials and methods

40 2.1 Materials

41 The chemical compositions and physical properties of the GGBS (from Hanson, UK) and CaO
42 (from Tarmac and Buxton Lime and Cement, UK) are summarised in Table 1. The dolomite
43 [CaMg(CO₃)₂] (DRB20) was supplied by IMERYS, UK and its elemental compositions determined
44 after acid dissolution with 1 mol/L HNO₃ by inductively coupled plasma optical emission
45 spectroscopy (ICP-OES, Perkin Elmer 7000) in triplicate, are also shown in Table 1. The Ca to Mg
46 molar ratio of the dolomite is 1.07. For calcination, approximately 50 g of raw dolomite was placed
47 in individual ceramic crucibles and heated in air to 800°C or 1000°C in an electric furnace. The
48
49
50
51
52
53
54
55
56
57
58
59
60
61
62
63
64
65

highest temperature was maintained for 1 h and then left to cool to room temperature. Two calcined products were obtained, namely D800 and D1000, referring to the products calcined at 800°C and 1000°C respectively, which were then stored in air tight plastic bags.

Table.1 Chemical compositions and physical properties of materials (from suppliers' datasheet AND * using

| ICP-OES) | | | |
|--|-------------|------------|----------------------|
| | GGBS | CaO | Dolomite(SD)* |
| Chemical composition | | | |
| SiO ₂ | 37.0 | 0.9 | 0.037 (0.00) |
| Al ₂ O ₃ | 13.0 | 0.13 | 0.001 (0.00) |
| CaO | 40.0 | 94.0 | 33.7 (0.17) |
| MgO | 8.0 | 0.5 | 18.9 (0.14) |
| K ₂ O | 0.6 | - | 0.011 (0.00) |
| Na ₂ O | 0.3 | - | 0.016 (0.00) |
| SO ₃ | 1.0 | 0.06 | NM |
| Fe ₂ O ₃ | - | 0.08 | 0.006 (0.00) |
| CaCO ₃ | - | 3.7 | - |
| CO ₂ | - | - | 47.3 (0.28) |
| LOI | - | 2.2 | - |
| Physical properties | | | |
| Specific surface area(m ² /g) | 0.49 | - | 1.70 |
| Bulk density(kg/m ³) | 1050 | 1020 | 900 |

NM-Not Measured

The calcined dolomite (D800 and D1000), as well as the raw dolomite, were characterised by XRD and TGA. The XRD patterns were collected using a Siemens D5000 X-ray diffractometer with a scanning range between 5° and 55° 2θ. The scanning speed of 1 s/step and resolution of 0.05°/step were applied. The TG measurements were carried out using a Perkin Elmer STA 6000 machine by heating the samples from 40°C to 1000°C at the rate of 10 °C/min. The XRD and TGA results are shown in Fig.1 and Fig.2, respectively.

The XRD pattern of the raw dolomite reveals that it also contained CaCO₃ (Fig.1) and is consistent with the Ca to Mg molar ratio being >1 as indicated by ICP-OES analysis (Table 1). The

1 TG curve of the raw dolomite indicates that its decarbonation process started at ~600°C and
2
3 terminated at ~850°C. It should be noted that this temperature range of decomposition could be
4
5 lower in comparison to that using a furnace due to the small amount of sample for the TGA test. The
6
7 decarbonation of dolomite is usually divided into two stages, but only one broad peak is observed in
8
9 the TG curve. Both XRD patterns and TG curves change significantly when the calcination
10
11 temperature increases from 800°C to 1000°C. Based on the weight loss measured by TGA, D1000
12
13 is estimated to contain 35.8% MgO, 54.6% CaO and 9.6% CaCO₃ [Ca(OH)₂ is converted into CaO]
14
15 while the composition of the D800 was difficult to determine because of the unknown fraction of
16
17 undecomposed dolomite and the overlap of decomposition reactions. It was measured that the
18
19 dolomite weight after calcination was approximately 72.3% of the initial weight when producing
20
21 D800. The low intensities of dolomite peaks in D800 XRD pattern were attributed to the high
22
23 relative intensity of calcite peak at 29.5°. The presence of Ca(OH)₂, which was also confirmed by
24
25 the weight loss between 350°C and 400°C (Fig.2), was caused by the ready hydroxylation of CaO
26
27 upon combining with moisture from ambient air [31].
28
29
30
31
32
33
34
35
36
37
38
39
40
41
42
43
44
45
46
47
48
49
50
51
52
53
54
55
56
57
58
59
60
61
62
63
64
65

1
2
3
4
5
6
7
8
9
10
11
12
13
14
15
16
17
18
19
20
21
22
23
24
25
26
27
28
29
30
31
32
33
34
35
36
37
38
39
40
41
42
43
44
45
46
47
48
49
50
51
52
53
54
55
56
57
58
59
60
61
62
63
64
65

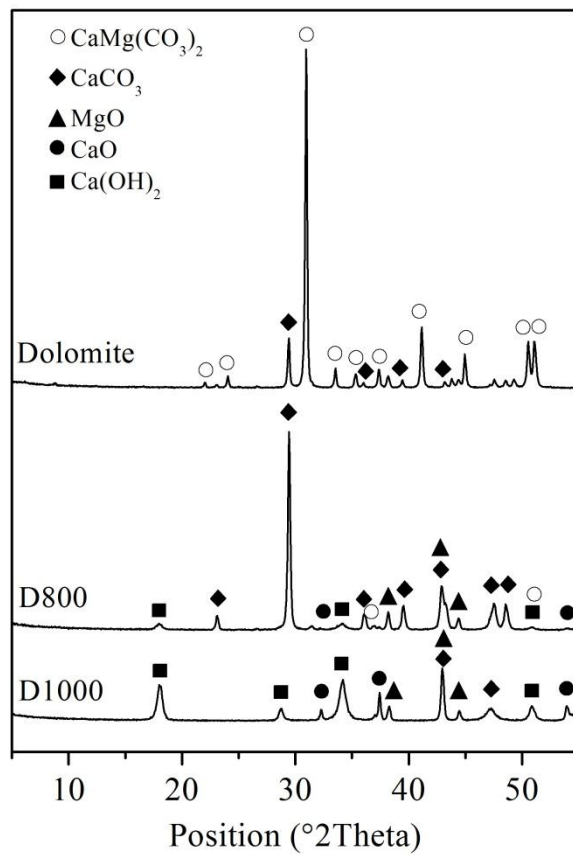


Fig.1 XRD patterns of the raw dolomite, D800 and D1000

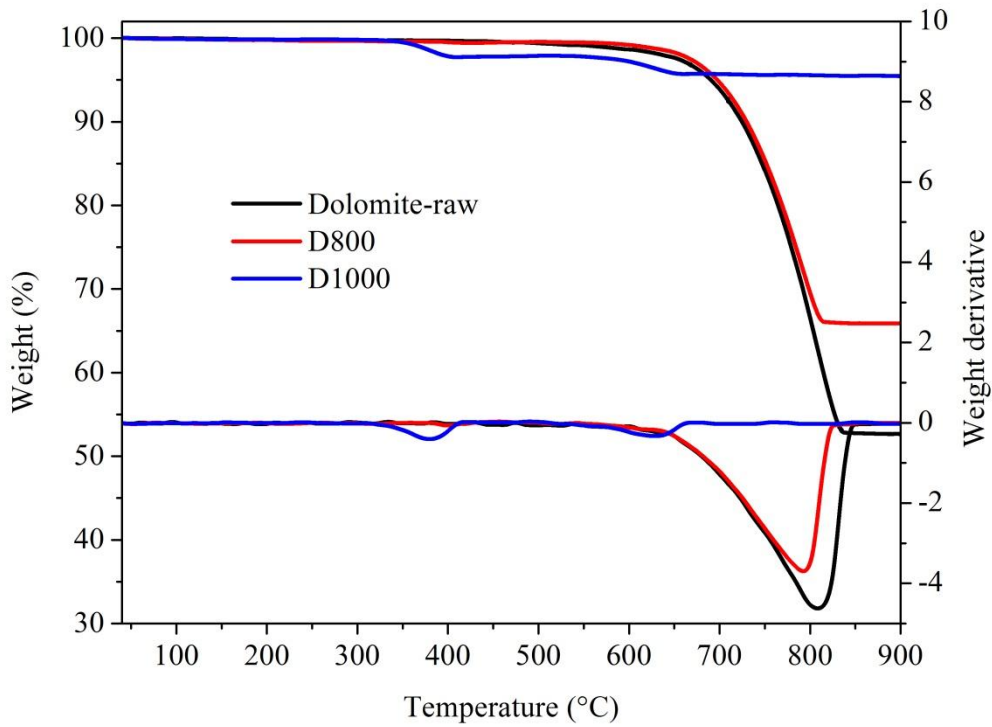


Fig.2 TG curves of the raw dolomite, D800 and D1000

2.2 Experimental methods

The content of the calcined dolomite in the test mixes was 10%, 12% and 15% and the control sample contained 10% CaO by weight. The dry materials were homogeneously mixed and deionised water was then added to obtain a 0.38 water/binder ratio. Paste samples were prepared using cube moulds, 40×40×40 mm, and covered with cling film to prevent water loss. After 24h, the samples were demoulded and stored in deionised water at the same temperature of 20±1°C. The nomenclature and compositions of the test pastes are presented in Table 2.

Table.2 Mix compositions of GGBS pastes

| Nomenclature | GGBS (%) | Activator (%) | | | water/binder ratio |
|--------------|----------|---------------|-------|-----|--------------------|
| | | D800 | D1000 | CaO | |
| D800-10 | 90 | 10 | - | - | 0.38 |
| D800-12 | 88 | 12 | - | - | 0.38 |
| D800-15 | 85 | 15 | - | - | 0.38 |
| D1000-10 | 90 | - | 10 | - | 0.38 |
| D1000-12 | 88 | - | 12 | - | 0.38 |
| D1000-15 | 85 | - | 15 | - | 0.38 |
| C10 | 90 | - | - | 10 | 0.38 |

The unconfined compressive strengths (UCS) were determined on triplicate paste cubes at 7, 28, 60, 90, 120 and 150 days at a constant load rate of 2400 N/sec. After the compression tests, the fractured paste samples were ground below 425 µm and fully mixed with deionised water at a liquid to solid ratio of 1 ml/g in airtight containers according to [32], which reported this method best simulates the pH of the pore solution. Pore solution pH readings were taken after 24 h using a Eutech 520 pH meter with an accuracy of 0.01 in duplicate and the average values are presented here. Hydration was arrested by immersing the samples in excess acetone and further dried by vacuum and oven. Some fractured pastes were finely ground below 75 µm for XRD and TGA, using the same equipment and parameters as stated in Section 2.1.

3. Results

3.1 Development of compressive strength

Fig.3 presents the compressive strength of the pastes up to 150 days. The use of D800 activator (10%) resulted in an ~11.5 MPa 7-day compressive strength, which was almost the same as that of the D1000 activated slag (~12.0 MPa) and was much lower than that of the control sample (~20.0 MPa). After 28 days, the D800 activated samples showed a significant increase in compressive strength and achieved ~25.9 MPa after 150 days of hydration, with the increase of strength became moderate after 120 days. The D1000 activator resulted in higher strengths than D800 at each age after 28 days and showed a final 150 days compressive strength of ~30.7 MPa.

In general, by increasing the dosage of D800 and D1000, higher compressive strengths were obtained. But the effect of activator dosage on the long term compressive strength was much more significant using D800 than using D1000. D800-15 showed 23.6% and 13.5% higher strength than D800-10 after 60 and 150 days, respectively, while only 2.9% and 7.4% higher strength was gained by increasing D1000 from 10% to 15% after the same time. This insignificant effect of D1000 on strength was more obvious when the dosage was higher than 12%. D1000-15 showed approximately the same strength as D1000-12 at each age.

In comparison to the control sample C10, D800-10 and D1000-10 showed lower compressive strength. After 7 days, the strength of D800-10 and D1000-10 was approximately 57.3% and 60.0% of C10, respectively, while these values increased to 69.1% and 86.5% after 90 days.

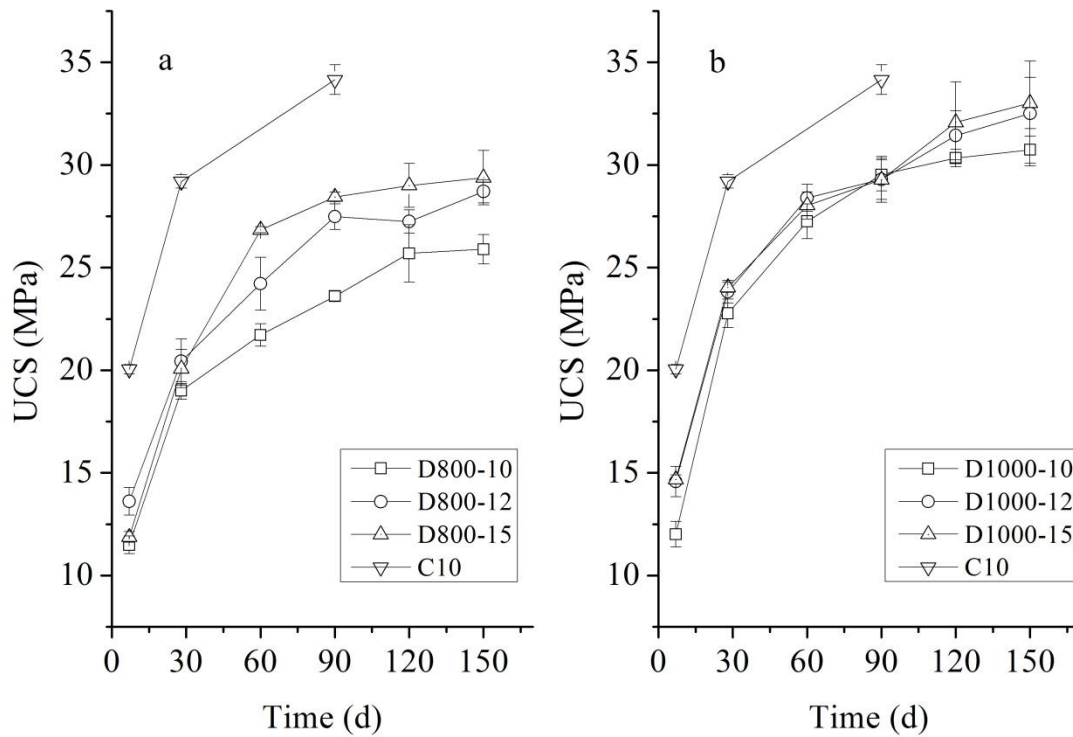


Fig.3 Unconfined compressive strength of activated GGBS pastes

3.2 pH of pore solution

According to the results of pH measurements given in Table 3, an average pH ~12.2 was obtained in the pastes using D800 in the early age (7 days) while in the pastes using D1000 pH averaged ~12.4. The control CaO sample induced the highest pH value (i.e. 12.6) at 7 days. In general, with the development of hydration reactions, the pH increased after 28 days, and D1000 gave still higher pH than D800. By increasing the dosage of activators, there were no clear changes in the pH, especially after 60 days, which was approximately 12.6 using D800 and 12.9 using D1000. For the control sample, pH was stable at 12.5-12.6 after 28 days and longer.

Table.3 pH of pore solution of activated GGBS

| Age | D800-10 | D800-12 | D800-15 | D1000-10 | D1000-12 | D1000-15 | C10 |
|-----|---------|---------|---------|----------|----------|----------|------|
| 7d | 12.3 | 12.2 | 12.2 | 12.5 | 12.3 | 12.4 | 12.6 |
| 28d | 12.1 | 12.6 | 12.7 | 12.4 | 12.9 | 12.9 | 12.5 |
| 60d | 12.7 | 12.6 | 12.7 | 13.0 | 12.9 | 13.0 | - |
| 90d | 12.7 | 12.4 | 12.5 | 13.0 | 12.9 | 12.8 | 12.6 |

3.3 Chemically bound water

By measuring the chemically bound water (CBW) content using TGA, the hydration degree of the slag can be estimated [33–35]. To obtain the bound water content, other research measured the weight loss of sample up to 650°C or higher [34,36–38]. In this study, the weight loss was determined up to 550°C because CaCO₃ decomposed at higher temperatures as characterised by TGA (discussed in Section 3.4). According to the measured content presented in Table 4, the nature of the activator was found to be a determining factor in weight loss within this temperature range. At a given dosage, D800 activated GGBS much more slowly (therefore lower hydration degree) than D1000, after each hydration period. The CBW amount was observed to be higher by increasing the dosage of the activators and the hydration period. The comparison between calcined dolomite activated slag and C10 revealed that both calcined dolomite activated GGBS more slowly than the CaO control sample.

Table.4 Chemically bound water content measured by TGA (weight loss over ignited weight of sample, %)

| Age | D800-10 | D800-12 | D800-15 | D1000-10 | D1000-12 | D1000-15 | C10 |
|-----|---------|---------|---------|----------|----------|----------|-----|
| 7d | 4.8 | 5.2 | 5.6 | 6.5 | 6.9 | 7.8 | 7.5 |
| 28d | 5.3 | 6.5 | 6.6 | 7.9 | 8.3 | 9.3 | 8.6 |
| 90d | 6.5 | 6.8 | 7.4 | 8.6 | 8.9 | 9.5 | 9.3 |

3.4 X-ray diffraction and thermogravimetric analysis

XRD patterns of selected samples (Fig.4) reveal the presence of C-S-H and hydrotalcite-like phases for all samples, correlating well with other works on individual MgO or CaO activated

1 GGBS [18,24,25]. A small amount of ettringite was also formed in all samples due to the presence
2
3 of sulphate in the slag. Highly intense characteristic peak of CaCO_3 at $\sim 29.5^\circ$ (overlap with C-S-H)
4
5 was detected in the D800 activated slag due to the high content of CaCO_3 in the activator. Since a
6
7 very small amount of CaCO_3 was detected by TGA in D1000 itself (Fig.2), the peaks of CaCO_3 in
8
9 the D1000 activated slag were mainly ascribed to the carbonation of hydration products, such as
10
11 $\text{Ca}(\text{OH})_2$, which was also observed in the XRD patterns of D1000 activated GGBS. By contrast, no
12
13 obvious $\text{Ca}(\text{OH})_2$ peaks were characterised in the D800 activated slag samples, probably due to
14
15 complete consumption during the hydration. Moreover, increasing dosage of both activators did not
16
17 induce new mineral patterns.
18
19
20
21
22
23
24

25 Both C-S-H (main weight loss between 80°C and 250°C) and hydrotalcite-like phases (weight
26
27 loss at $\sim 200^\circ\text{C}$ and between 360°C and 440°C) were detected by TGA in all pastes (Fig.5 and Fig.6).
28
29 The weight loss after 600°C was due essentially to decarbonation of CaCO_3 from the raw materials
30
31 and/or the carbonated hydration products during curing. Decomposition of $\text{Ca}(\text{OH})_2$ was identified
32
33 at $\sim 450^\circ\text{C}$, shown in Fig.6, consisting well with the XRD patterns (Fig.4).
34
35
36
37
38
39
40
41
42
43
44
45
46
47
48
49
50
51
52
53
54
55
56
57
58
59
60
61
62
63
64
65

1
2
3
4
5
6
7
8
9
10
11
12
13
14
15
16
17
18
19
20
21
22
23
24
25
26
27
28
29
30
31
32
33
34
35
36
37
38
39
40
41
42
43
44
45
46
47
48
49
50
51
52
53
54
55
56
57
58
59
60
61
62
63
64
65

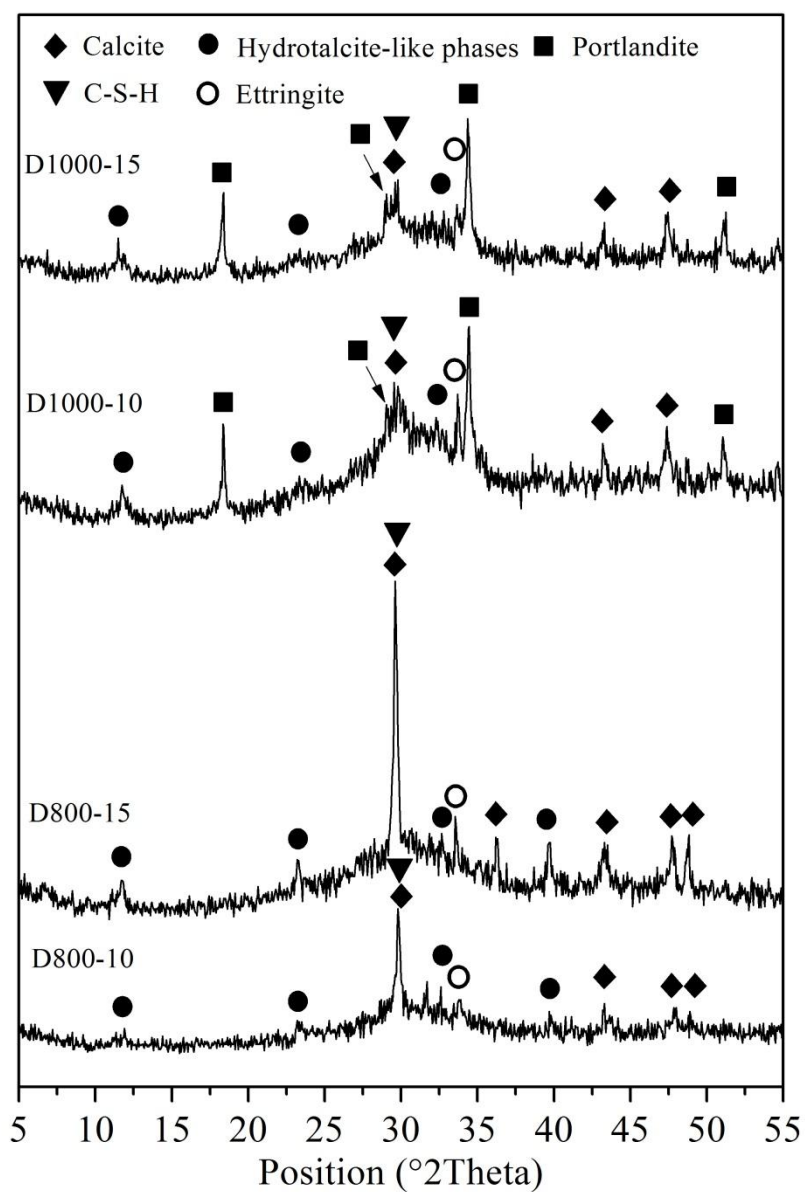


Fig.4 Comparison of the XRD patterns of selected samples after 28 days

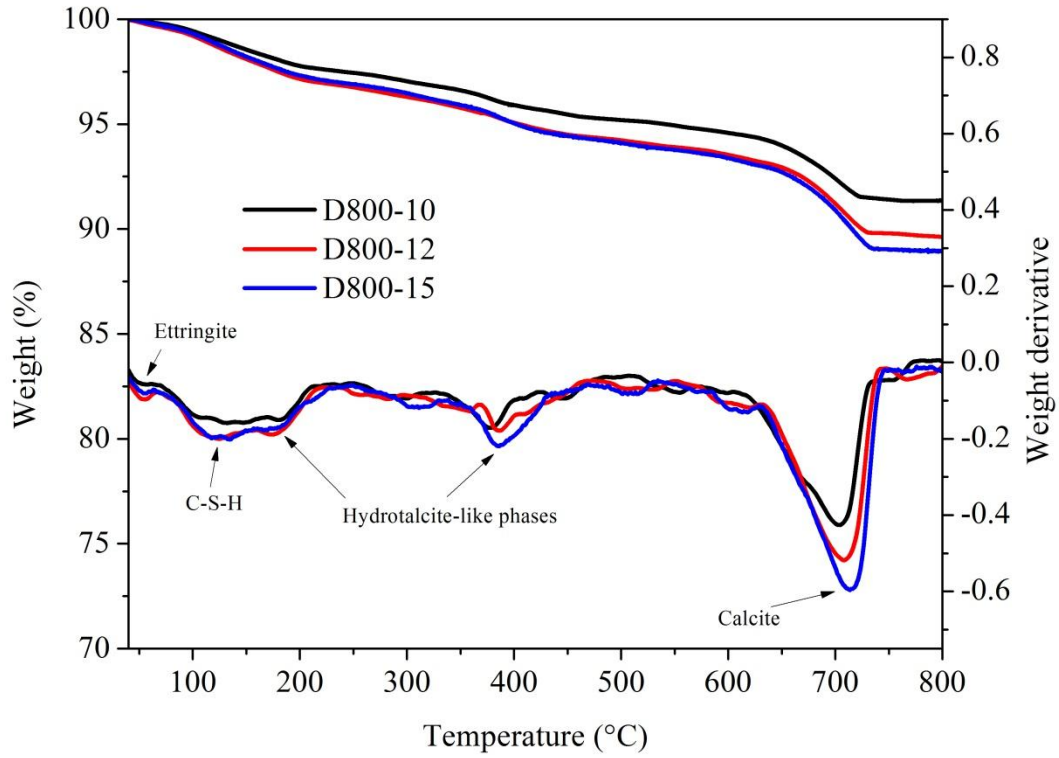


Fig.5 TG curves of D800-GGBS pastes after 28 days

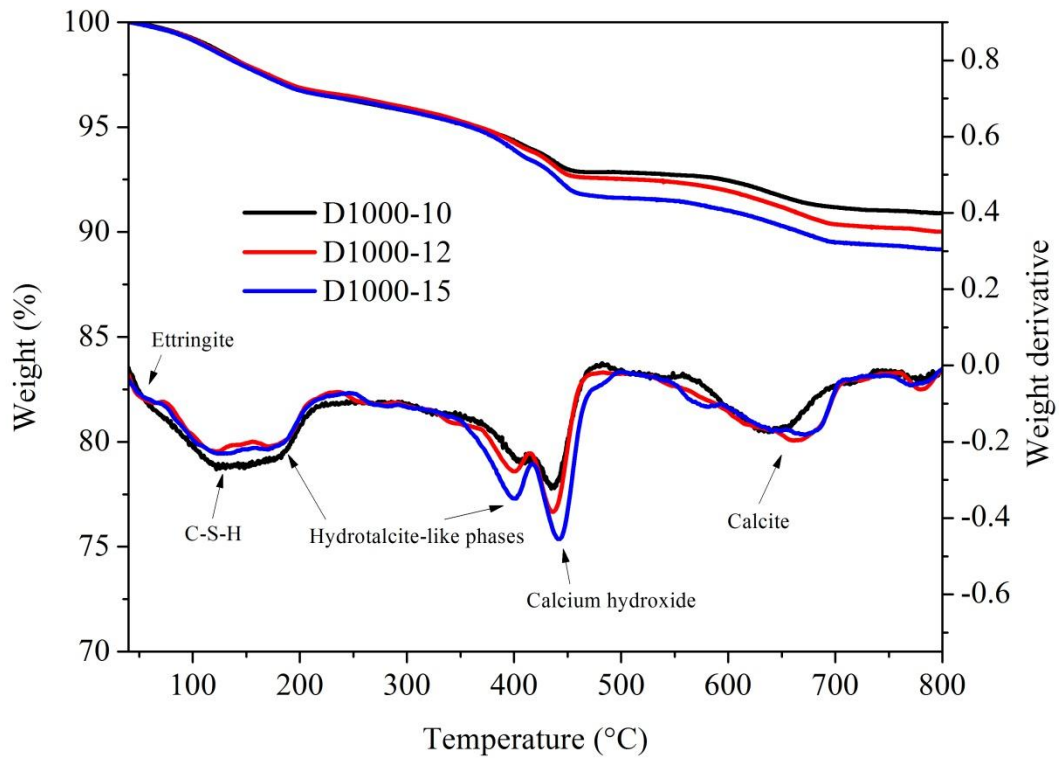


Fig.6 TG curves of D1000-GGBS pastes after 28 days

4. Discussion

The compressive strength result showed that both D800 and D1000 activated slag had lower strength than CaO, up to 90 days (Fig.3). In order to recognise the efficiency of slag activation by using calcined dolomite, the comparison of compressive strength of calcined dolomite activated slag to reactive MgO or Portland cement (PC) activated slag was also made (Fig.7). A reactive MgO and CEM I 52.5N PC were used. The chemical composition and physical properties of MgO and PC powders are given in Table 5. The reactivity of MgO is 100 s determined by the acetic acid test according to Shand [39] and is categorised as a medium reactive MgO. The preparation method of MgO or PC activated slag samples was exactly the same as mentioned in Section 2.2. The dosage of activator and water to binder ratio was also 10% and 0.38, respectively.

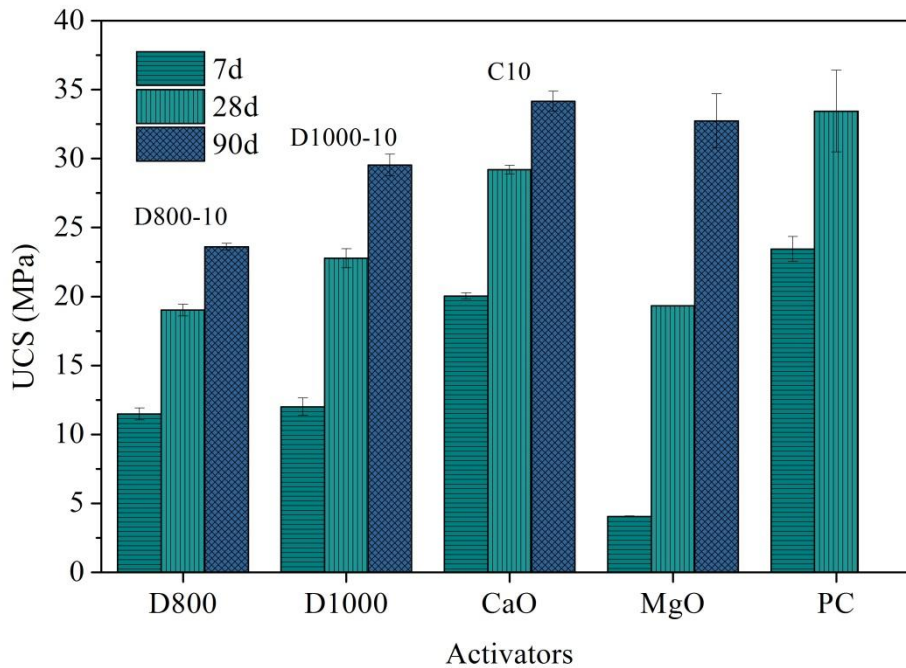


Fig.7 Strengths of activated slag by using different activators. Activator dosage controlled at 10%, w/b ratio controlled at 0.38 and all samples cured in water.

Table.5 Chemical compositions and physical property of reactive MgO and PC (from suppliers' datasheet)

| | MgO | PC |
|---|-------------|-------------|
| Chemical composition | | |
| SiO ₂ | 0.9 | 19.47 |
| Al ₂ O ₃ | 0.22 | 4.75 |
| CaO | 0.9 | 63.16 |
| MgO | 93.4 | 1.43 |
| K ₂ O | - | 0.62 |
| Na ₂ O | - | 0.28 |
| SO ₃ | - | 2.68 |
| Fe ₂ O ₃ | 0.5 | 3.43 |
| Cl | - | 0.0094 |
| LOI | - | 3.26 |
| Specific surface area(m²/g) | 9.00 | 0.40 |

Fig. 7 reveals that calcined dolomite activated slag has much better mechanical performance than MgO activated slag in the early age but lower strengths after 90 days. The compressive strength of D800-10 and D1000-10 is about 284% and 297% strength of MgO activated slag, respectively, after 7 days. After 28 days, the strength of D800-10 is very close to MgO activated slag while D1000-10 is also only 117.8% of MgO activated slag. After 90 days, however, the strength of calcined dolomite activated slag is observed to be lower than MgO alone activated slag. It has been found that, although reactive MgO showed a slow acceleration of slag in the early age, it can induce much better mechanical performance of slag pastes after 28 days and longer, due to the formation of voluminous hydrotcalcite-like phases [24,25]. Nevertheless, it is reasonable to conclude that, to substitute calcined dolomite for MgO can greatly accelerate the hydration process in the early age, although not necessarily induce better mechanical performance in the later ages.

In case of the activator PC, calcined dolomite activated samples also have lower strength than PC activated slag up to 28 days. In fact, PC induces the highest strength among all other activators.

1 It can be demonstrated by the type of PC (i.e. CEM I 52.5N), which is often used where there is a
2
3 requirement of early strength.
4

5
6 It should be noted that the nature of MgO (i.e. reactivity, fineness), which depends on the
7
8 manufacturing process, has significant impact on the strength of activated slag according to the
9
10 literature [40]. Similarly, the strengths of PC activated slag also vary with the type of PC used.
11
12 Therefore, in case of evaluating the activation efficiency of calcined dolomite, the comparison to
13
14 other activators shown in Fig.7 should be reserved .
15
16
17
18
19

20 It has been found that, in the early age, the addition of CaO can effectively accelerate the
21
22 hydration of MgO-GGBS blends, therefore giving higher compressive strengths than slag pastes
23
24 activated by MgO alone[25]. In addition, the paste strength was in positive correlation with the
25
26 CaO/MgO weight ratio, although this correlation become less apparent when CaO/MgO was higher
27
28 than 1 [25]. Based on the composition analysis of D800 and D1000, it can be deduced that D800 has
29
30 lower amount of CaO and with a CaO/MgO<1 by weight while D1000 has more CaO and with
31
32 CaO/MgO≈1.5 by weight. However, the D800 activated samples revealed similar strengths to the
33
34 D1000 activated ones. The reasons can be demonstrated by the reactivity of MgO and the role
35
36 played by CaCO₃. Owing to the lower calcination temperature, the MgO in D800, which was of
37
38 higher reactivity [30,39], can produce higher early age compressive strengths. Jin et al. [23]
39
40 investigated the hydration of different MgO activated GGBS pastes and concluded that reactive
41
42 MgO with higher reactivity resulted in higher early strength. The amount of chemically bound water
43
44 given in Table 4, however, indicates that the extent of hydration of the D800 activated slags was still
45
46 lower than that of the D1000 activated samples, suggesting the considerable amount of CaCO₃ in
47
48 D800 sample may also contribute to the early strength of pastes. Previous studies on the role of
49
50
51
52
53
54
55
56
57
58
59
60
61
62
63
64
65

limestone in accelerating strengths of slag cement have indicated that CaCO_3 powder can improve the early compressive strength and tighten pore structure at early age [19,41]. Therefore the pastes in this study showed higher strengths in spite of the lower degree of hydration.

Fig.8 illustrates the relation of CBW amount and the compressive strengths up to 90 days, regardless of the dosage of D800 or D1000 used. Pore filling effect of CaCO_3 from calcined dolomite was obvious up to 90 days because with the same amount of CBW, the samples activated by D800 showed higher strengths than those by D1000. On the other hand, when the dosage of calcined dolomite was given, D1000 always produced larger amounts of hydration products (mainly C-S-H gel and hydrotalcite-like phases) (Table 4, Fig.5 and Fig.6) after 28 days and longer, which explains the higher compressive strengths.

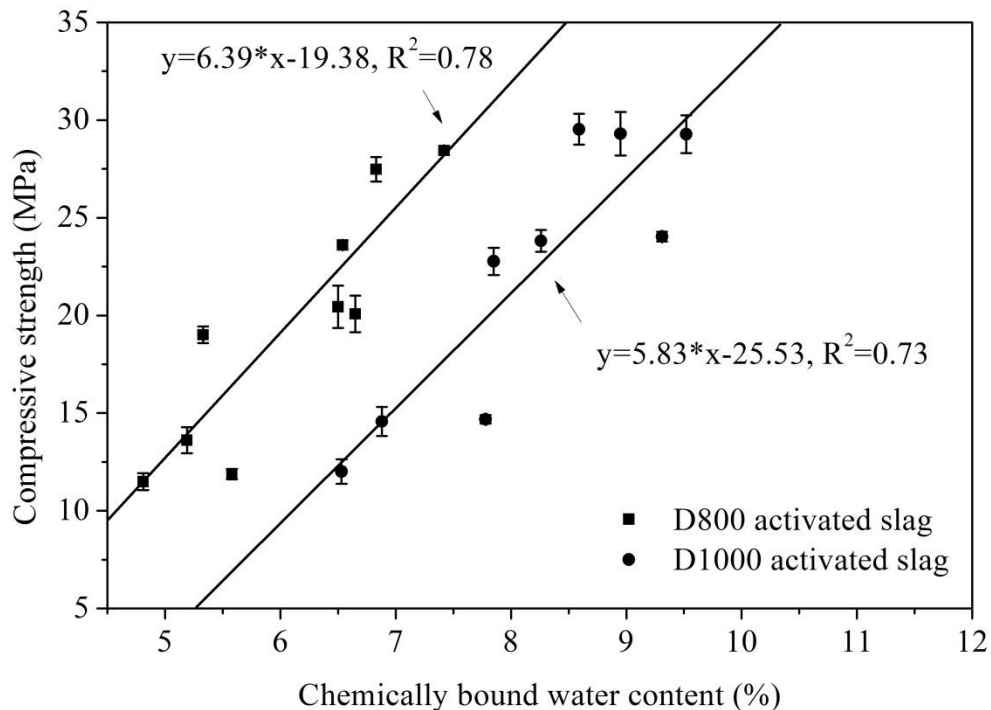


Fig.8 Relation of the chemically bound water content and the compressive strength

If the raw dolomite completely decomposed, MgO would account for 35.8% by weight of calcined products, according to the compositions of dolomite given in Table 1. In this case, 10%

1 D800 in samples contained less than 3.6% MgO while 15% D800 in samples contained less than
2
3 5.4% MgO by weight, owing to incomplete decomposition. As a consequence, by increasing the
4
5 dosage of D800 to 15%, an apparent strength enhancement was observed since the suggested
6
7 optimum content of individual MgO in the blends was ~10% according to Yi et al. [24]. However,
8
9 arbitrarily increasing the dosage should not be encouraged because negative effects of limestone on
10
11 mechanical properties or durability of Portland cement starts to be observed when the amount of
12
13 limestone per mass of cement exceeds 10-15% [42]. The inconspicuous increase in compressive
14
15 strength after increasing the dosage of D1000 could be attributed to the effect of $\text{Ca}(\text{OH})_2$ in the late
16
17 ages, although the MgO content in D1000 was closer to the optimum. It has been reported that
18
19 although $\text{Ca}(\text{OH})_2$ increased early age compressive strength, it slightly decreased the later age
20
21 strengths in many cases [5,19,43].
22
23
24
25
26
27
28
29
30

31 Prior research has indicated that pH has a significant effect on the hydration process of
32
33 activated slag systems and also the nature of the products generated [19,44,45]. Higher pH
34
35 environments usually induce better slag activation and higher mechanical strength [19,44,46]. In
36
37 addition, the pH should be ≥ 11.5 in order to effectively activate the hydration of slag [45]. As
38
39 indicated in Table 3, the pH values of the D800 activated slag (12.1-12.7) and the D1000 activated
40
41 slag (12.2-13.0) suggest that both the calcined dolomites used in this study could effectively
42
43 activate the slag. In comparison to D800, the higher pH of D1000 resulted in a higher slag
44
45 activation at each age, as indicated by the higher chemically bound water content in Table 4.
46
47
48 However, it was observed that C10 did not show high pH at later ages but still had higher extent of
49
50 hydration. This can be explained by the higher pH (i.e. 12.6) in the early age therefore a larger
51
52 amount of slag could have reacted, hence higher extent of reaction. It should be noted that the
53
54
55
56
57
58
59
60
61
62
63
64
65

1 maintenance of pH depends on the amount of Ca(OH)_2 accessible to the pore solution, rather than
2
3 its amount in the sample [47]. In this case, the small difference in pH values of samples using
4
5 different dosages of activators after 60 days could be illustrated by a similar amount of accessible
6
7 Ca(OH)_2 in these samples. On the other hand, the relatively lower pH of C10 after 28 days
8
9 suggests a larger content of accessible Ca(OH)_2 in the sample than the calcined dolomite activated
10
11 samples. The equilibrium pH of Ca(OH)_2 is approximate 12.5-12.6 and the continuous release of
12
13 Ca^{2+} ion could maintain the pH at this level, even though the sample might suffer from **minor**
14
15 **carbonation during curing [44,48]**, which could induce a slight decrease in pH by consuming Ca^{2+}
16
17 and OH^- ions. In case of D800-12, D800-15 and D1000-15, carbonation appeared to cause a
18
19 decrease of pH after 90 days.
20
21
22
23
24
25
26

27
28 Based on the results presented in this paper, it is shown that GGBS activated by dolomite
29
30 calcined at higher temperature (**with** complete decomposition) exhibited slightly higher strength
31
32 and higher extent of hydration than GGBS activated by dolomite calcined at lower temperature
33
34 (incomplete decomposition). On the other hand, **the** incomplete decomposition of dolomite at lower
35
36 calcination temperature is associated with lower energy consumption and lower CO_2 emission,
37
38 which makes it more economical and environmentally friendly. The relatively lower strength could
39
40 be remedied by **appropriately** increasing the dosage. **The durability issues of calcined dolomite**
41
42 **activated slags are of great importance for its future application. Among others, the resistance of**
43
44 **calcined dolomite activated slags to chemical attacks, such as sulphate and acid attack, and**
45
46 **carbonation will be presented elsewhere.**
47
48
49
50
51
52
53
54
55

56 **5. Conclusions**

57
58 Natural dolomite was calcined at 800 and 1000°C under air, and was investigated as a potential
59
60

1 activator for GGBS. Based on the results obtained by a range of tests, the following conclusions can
2
3 be drawn.
4

5
6 1. D800 and D1000 were characterised using XRD and TGA. For D800, only 72.3% of the
7
8 natural dolomite was decomposed, while D1000 consisted of 35.8% MgO, 54.6% CaO and 9.6%
9
10 CaCO₃. The newly generated CaO was readily hydrated in ambient air, whilst MgO was relatively
11
12 stable for both calcined dolomite samples.
13
14

15
16 2. Both calcined dolomites in this study can effectively activated slag. The strengths of
17
18 calcined dolomite activated slag were lower than CaO alone activated slag, at the dosage of 10%.
19
20
21 To substitute calcined dolomite for MgO can greatly increase the strength of activated slag in the
22
23 early age, although not necessarily induce better mechanical performance in the later ages. In
24
25 addition, calcined dolomites activated slag samples have lower strengths than PC (CEM I 52.5N)
26
27 activated slag in this study.
28
29
30
31

32
33 3. The extent of hydration was determined by TG analysis. At a given dosage, D1000 induced
34
35 higher slag hydration degrees than D800 at each curing age. Both D800 and D1000 showed slower
36
37 activation of slag than CaO alone at the dosage of 10% by weight.
38
39
40

41
42 4. GGBS activated by both activators showed similar early age compressive strengths due to
43
44 the higher reactivity of MgO and the filler effect of CaCO₃ contained in D800, while at the later age
45
46 (after 28 days), the D1000 activated slag showed much higher strengths. While producing the same
47
48 amount of chemically bound water in the paste, the D800 activated slag showed higher strengths.
49
50

51
52 5. By increasing the dosage of activator, higher compressive strengths were obtained.
53
54 Significant enhancements were observed when using D800 while only small increases were
55
56 detected when using D1000.
57
58
59
60

1 6. The main hydration products C-S-H and hydrotalcite-like phases were observed by XRD
2
3 and TGA. Ca(OH)₂ was only detected in the D1000 activated pastes.
4
5

6 **Acknowledgements**

7
8 The work presented in this paper was carried out at Department of Engineering, University of
9
10 Cambridge, in the academic year 2012-2013 when the first author was a visiting researcher there.
11
12 The visit was funded by the China Scholarship Council and the Scientific Research Foundation of
13
14 the Graduate School of Nanjing University (No.2012CL11), which are greatly appreciated. The
15
16 financial support for the PhD studentship of the second author from the Cambridge Trust and the
17
18 China Scholarship Council is also much appreciated. Many thanks to Dr. Sue Struthers for her
19
20 contribution to language improvement.
21
22
23
24
25
26
27
28
29
30

31 **References**

- 32
33
34 [1] Juenger MCG, Winnefeld F, Provis JL, Ideker JH. Advances in alternative cementitious
35 binders. *Cem Concr Res* 2011;41:1232–43.
36
37
38 [2] Anand S, Vrat P, Dahiya RP. Application of a system dynamics approach for assessment and
39 mitigation of CO₂ emissions from the cement industry. *J Environ Manage* 2006;79:383–98.
40
41
42 [3] Provis JL, van Deventer JSJ. Alkali Activated Materials: State-of-the-Art Report, RILEM TC
43 224-AAM. Dordrecht: Springer Netherlands; 2014.
44
45
46 [4] Bakharev T, Sanjayan JG, Cheng Y-B. Alkali activation of Australian slag cements. *Cem*
47 *Concr Res* 1999;29:113–20.
48
49
50 [5] Collins FG, Sanjayan JG. Workability and mechanical properties of alkali activated slag
51 concrete. *Cem Concr Res* 1999;29:455–8.
52
53
54 [6] Fernández-Jiménez A, Palomo J, Puertas F. Alkali-activated slag mortars: mechanical strength
55 behaviour. *Cem Concr Res* 1999;29:1313–21.
56
57
58 [7] Bakharev T, Sanjayan JG, Cheng Y-B. Sulfate attack on alkali-activated slag concrete. *Cem*
59 *Concr Res* 2002;32:211–6.
60
61
62
63
64
65

- 1
2
3
4
5
6
7
8
9
10
11
12
13
14
15
16
17
18
19
20
21
22
23
24
25
26
27
28
29
30
31
32
33
34
35
36
37
38
39
40
41
42
43
44
45
46
47
48
49
50
51
52
53
54
55
56
57
58
59
60
61
62
63
64
65
- [8] Bakharev T, Sanjayan J., Cheng Y-B. Resistance of alkali-activated slag concrete to acid attack. *Cem Concr Res* 2003;33:1607–11.
- [9] Roy D, Jiang W, Silsbee M. Chloride diffusion in ordinary, blended, and alkali-activated cement pastes and its relation to other properties. *Cem Concr Res* 2000;30:1879–84.
- [10] Shi C, Xie P. Interface between cement paste and quartz sand in alkali-activated slag mortars. *Cem Concr Res* 1998;28:887–96.
- [11] Brough AR, Atkinson A. Automated identification of the aggregate–paste interfacial transition zone in mortars of silica sand with Portland or alkali-activated slag cement paste. *Cem Concr Res* 2000;30:849–54.
- [12] Shi C, Krivenko P, Roy D. *Alkali-activated cements and concretes*. Abingdon,UK: Taylor & Francis; 2006.
- [13] Wang SD, Pu XC, Scrivener KL, Pratt PL. Alkali-activated slag cement and concrete: a review of properties and problems. *Adv Cem Res* 1995;7:93–102.
- [14] Rashad AM. A comprehensive overview about the influence of different additives on the properties of alkali-activated slag – A guide for Civil Engineer. *Constr Build Mater* 2013;47:29–55.
- [15] Gong C, Yang N. Effect of phosphate on the hydration of alkali-activated red mud–slag cementitious material. *Cem Concr Res* 2000;30:1013–6.
- [16] Yang K-H, Song J-K, Ashour AF, Lee E-T. Properties of cementless mortars activated by sodium silicate. *Constr Build Mater* 2008;22:1981–9.
- [17] Yang K-H, Cho A-R, Song J-K, Nam S-H. Hydration products and strength development of calcium hydroxide-based alkali-activated slag mortars. *Constr Build Mater* 2012;29:410–9.
- [18] Kim MS, Jun Y, Lee C, Oh JE. Use of CaO as an activator for producing a price-competitive non-cement structural binder using ground granulated blast furnace slag. *Cem Concr Res* 2013;54:208–14.
- [19] Wang S, Scrivener K, Pratt P. Factors affecting the strength of alkali-activated slag. *Cem Concr Res* 1994;24:1033–43.
- [20] Yang K-H, Cho A-R, Song J-K. Effect of water–binder ratio on the mechanical properties of calcium hydroxide-based alkali-activated slag concrete. *Constr Build Mater* 2012;29:504–11.
- [21] Shen W, Wang Y, Zhang T, Zhou M, Li J, Cui X. Magnesia modification of alkali-activated slag fly ash cement. *J Wuhan Univ Technol Sci Ed* 2011;26:121–5.

- 1
2
3
4
5
6
7
8
9
10
11
12
13
14
15
16
17
18
19
20
21
22
23
24
25
26
27
28
29
30
31
32
33
34
35
36
37
38
39
40
41
42
43
44
45
46
47
48
49
50
51
52
53
54
55
56
57
58
59
60
61
62
63
64
65
- [22] Li X. Mechanical properties and durability performance of reactive magnesium cement concrete, PhD thesis. University of Cambridge, UK, 2012.
- [23] Jin F, Abdollahzadeh A, Al-Tabbaa A. Effect of different MgO on the hydration of MgO-activated granulated ground blastfurnace slag paste. Proc. Int. Conf. Sustain. Constr. Mater. Technol., Kyoto, Japan: 2013.
- [24] Yi Y, Liska M, Al-Tabbaa A. Properties and microstructure of GGBS–magnesia pastes. Adv Cem Res 2013:1–9.
- [25] Gu K. Experimental study on engineering properties of MgO-CaO mixtures activated ground granulated blastfurnace slag, PhD Thesis. Nanjing University, 2014.
- [26] Warren J. Dolomite: occurrence, evolution and economically important associations. Earth-Science Rev 2000;52:1–81.
- [27] Huang XP, Zhang Q, Guo SY, Wang GW. The Present State and Future Outlook of the Exploitation & Utilization of Magnesium Resource in Sea Water and Brine about Our Country. Sea-Lake Salt Chem Ind 2004;33:1–6.
- [28] Maitra S, Choudhury a., Das HS, Pramanik MJ. Effect of compaction on the kinetics of thermal decomposition of dolomite under non-isothermal condition. J Mater Sci 2005;40:4749–51.
- [29] Xu L, Deng M. Dolomite used as raw material to produce MgO-based expansive agent. Cem Concr Res 2005;35:1480–5.
- [30] Sasaki K, Qiu X, Hosomomi Y, Moriyama S, Hirajima T. Effect of natural dolomite calcination temperature on sorption of borate onto calcined products. Microporous Mesoporous Mater 2013;171:1–8.
- [31] Caceres PG, Attiogbe EK. Thermal decomposition of dolomite and the extraction of its constituents. Miner Eng 1997;10:1165–76.
- [32] Hidalgo A, Garcia JL, Aloson MC, Fernandez-Luco L, Andrade C. Testing methodology for pH determination of cementitious materials. application to low pH binders for use in HLNWR. In: Bäckblom G, editor. 2nd Work. R&D low-pH Cem. a Geol. Repos., Madrid: 2005.
- [33] Bhatt J. A review of the application of thermal analysis to cement-admixture systems. Thermochim Acta 1991;189:313–50.
- [34] Escalante-García JI, Fuentes AF, Gorokhovskiy A, Fraire-Luna PE, Mendoza-Suarez G. Hydration Products and Reactivity of Blast-Furnace Slag Activated by Various Alkalis. J Am Ceram Soc 2003;86:2148–53.

- 1
2
3
4
5
6
7
8
9
10
11
12
13
14
15
16
17
18
19
20
21
22
23
24
25
26
27
28
29
30
31
32
33
34
35
36
37
38
39
40
41
42
43
44
45
46
47
48
49
50
51
52
53
54
55
56
57
58
59
60
61
62
63
64
65
- [35] Gruskovnjak A, Lothenbach B, Winnefeld F, Münch B, Figi R, Ko S-C, et al. Quantification of hydration phases in supersulfated cements: review and new approaches. *Adv Cem Res* 2011;23:265–75.
- [36] Escalante JI, Gómez LY, Johal KK, Mendoza G, Mancha H, Méndez J. Reactivity of blast-furnace slag in Portland cement blends hydrated under different conditions. *Cem Concr Res* 2001;31:1403–9.
- [37] Ben Haha M, Lothenbach B, Le Saout G, Winnefeld F. Influence of slag chemistry on the hydration of alkali-activated blast-furnace slag — Part I: Effect of MgO. *Cem Concr Res* 2011;41:955–63.
- [38] Ben Haha M, Lothenbach B, Le Saout G, Winnefeld F. Influence of slag chemistry on the hydration of alkali-activated blast-furnace slag — Part II: Effect of Al₂O₃. *Cem Concr Res* 2012;42:74–83.
- [39] Shand MA. *The chemistry and technology of magnesia*. Hoboken, New Jersey: John Wiley & Sons; 2006.
- [40] Jin F, Gu K, Abdollahzadeh A, Al-Tabbaa A. Effect of different reactive MgOs on the hydration of MgO-activated ground granulated blastfurnace slag paste. *J Mater Civ Eng* 2014;doi:10.1061/(ASCE)MT.1943-5533.0001009.
- [41] Mun KJ, So SY, Soh YS. The effect of slaked lime, anhydrous gypsum and limestone powder on properties of blast furnace slag cement mortar and concrete. *Constr Build Mater* 2007;21:1576–82.
- [42] Lothenbach B, Le Saout G, Gallucci E, Scrivener K. Influence of limestone on the hydration of Portland cements. *Cem Concr Res* 2008;38:848–60.
- [43] Shi C, Day R. Early strength development and hydration of alkali-activated blast furnace slag/fly ash blends. *Adv Cememnt Res* 1999;11:189–96.
- [44] Roy A, Schilling PJ, Eaton HC, Malone PG, Brabston WN, Wakeley LD. Activation of Ground Blast-Furnace Slag by Alkali-Metal and Alkaline-Earth Hydroxides. *J Am Ceram Soc* 1992;75:3233–40.
- [45] Song S, Jennings H. Pore solution chemistry of alkali-activated ground granulated blast-furnace slag. *Cem Concr Res* 1999;29:159–70.
- [46] Ben Haha M, Le Saout G, Winnefeld F, Lothenbach B. Influence of activator type on hydration kinetics, hydrate assemblage and microstructural development of alkali activated blast-furnace slags. *Cem Concr Res* 2011;41:301–10.

- 1
2
3
4 [47] Atkins M, Glasser FP. Application of portland cement-based materials to radioactive waste
5 immobilization. Waste Manag 1992;12:105–31.
6
7
8
9
10
11
12
13
14 [48] Criado M, Palomo a, Fernandezjimenez a. Alkali activation of fly ashes. Part 1: Effect of
15 curing conditions on the carbonation of the reaction products. Fuel 2005;84:2048–54.
16
17
18
19
20
21
22
23
24
25
26
27
28
29
30
31
32
33
34
35
36
37
38
39
40
41
42
43
44
45
46
47
48
49
50
51
52
53
54
55
56
57
58
59
60
61
62
63
64
65

The list of captions for all tables:

1. Table.1 Chemical compositions and physical properties of materials (from suppliers' datasheet AND * using ICP-OES)
2. Table.2 Mix compositions of GGBS pastes
3. Table.3 pH of pore solution of activated GGBS
4. Table.4 Chemically bound water content measured by TGA (weight loss over ignited weight of sample, %)
5. Table.5 Chemical compositions and physical property of reactive MgO and PC (from suppliers' datasheet)

The list of captions for all figures:

1. Fig.1 XRD patterns of raw dolomite, D800 and D1000
2. Fig.2 TG curves of raw dolomite, D800 and D1000
3. Fig.3 Unconfined compressive strength of activated GGBS pastes
4. Fig.4 Comparison of XRD patterns of selected samples after 28 days
5. Fig.5 TG curves of D800-GGBS pastes after 28 days
6. Fig.6 TG curves of D1000-GGBS pastes after 28 days
7. Fig.7 Strengths of activated slag by using different activators. Activator dosage controlled at 10%, w/b ratio controlled at 0.38 and all samples cured in water.
8. Fig.8 Relation of chemically bound water content and compressive strength